Tuning magnetoelectric coupling in ferrite-ferroelectric system of $CoFe_2O_4$-$BaTiO_3$ using carbon combustion process

C. Trevino De Leo[a], G.C. Dannangoda[a], M.A. Hobosyan[a], J.T. Held[b], F. Safi Samghabadi[c], M. Khodadadi[c], D. Litvinov[c], K.A. Mkhoyan[b], K.S. Martirosyan[a]

[a]Advanced Nanoscience Laboratory, Department of Physics and Astronomy, University of Texas Rio Grande Valley, Brownsville, TX, 78520, USA
[b]Department of Chemical Engineering and Materials Science, University of Minnesota, Minneapolis, MN, 55455, USA
[c]Materials Science & Engineering and Electrical & Computer Engineering, University of Houston, Houston, TX, 77204, USA

Introduction and Experimental Methods

- Carbon combustion synthesis of oxides (CCSO) is a quick and energy efficient method for producing matrix structure nanocomposites.
- The exothermic oxidation of carbon nanoparticles with a generates a self-propagating thermal wave with peak temperatures of up to 1000 ◦C.
- The thermal front rapidly propagates through the mixture of solid reactants and results in localized hot-spot sintering of magnetoelectric (ME) phases to form a nanocomposite structure.
- The individual electromagnetic properties of the materials (ferromagnetic $CoFe_2O_4$ and ferroelectric $BaTiO_3$) result into a ME coupling on cobalt ferrite–barium titanate ceramic composites after ignition.
- Reactants mixture contains 200 nm $BaTiO_3$ and 30 nm $CoFe_2O_4$ at equimolar ratios with different concentrations of Carbon Acetylene with particle size of 5 nm.
- The reagents were mixed with a roller ball milling for 3 h.
- The powder was placed on a porous alumina substrate with a feed line of oxygen from top to bottom. Thermocouples at top, center and bottom recorded the temperature variation.
- Heat propagates downwards at a velocity of 0.1-4 mm/s through the solid mixture.

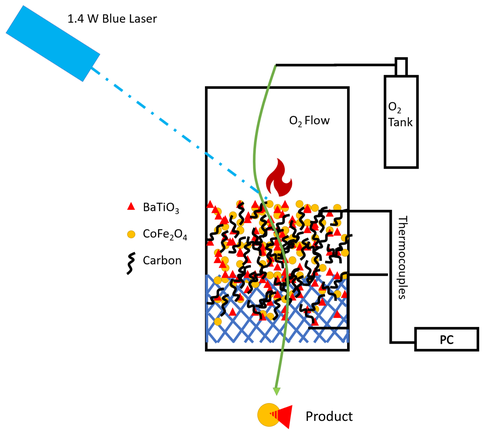

Fig. 1. Schematics of CCSO for magnetoelectric coupling of $CoFe_2O_4$ and $BaTiO_3$. The hot spot sintered intersection between the two particles is shown.

Thermodynamic Analysis

- Thermodynamic analysis is critical to evaluate the energetic capacity of the system, predict the adiabatic temperature and anticipate the condensed and liquid phase concentrations, which will determine the particle sintering potential and combustion front propagation.

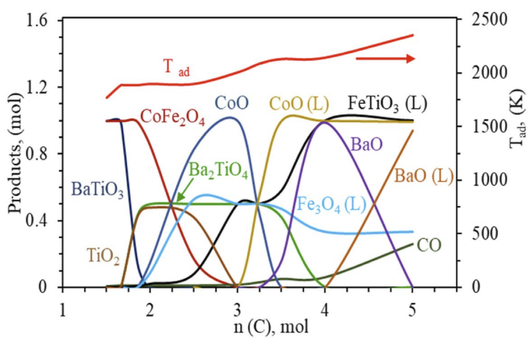

Fig. 2. Product composition dependence on carbon concentration for the system $CoFe_2O_4$ -$BaTiO_3$-n(C + O_2) and adiabatic temperature of combustion with n_i = 0.5 + 0.25i increments. Thermodynamic calculations were performed with "Thermo" software. (L) represents the liquid phases in the system, whereas other species are in solid or gas phase. Maximum sintering potential is determined at ~4.5 mol C where more liquid phases are present.

Calorimetry and Thermogravimetric Data

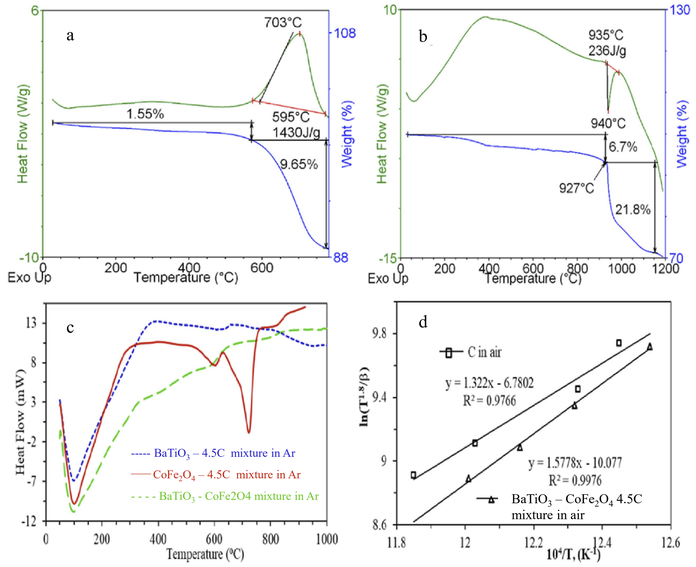

Fig. 3. (a) DSC-TGAs of $BaTiO_3$ – $CoFe_2O_4$ - nC (n=4.5) mixture in air vs (b) mixture in Argon (Ar); (c) DSCs of individual components under CCSO versus mixture all in Ar; (d) Arrhenius plot for the carbon nanoparticles combustion (⊟), and $BaTiO_3$–$CoFe_2O_4$- 4.5C system combustion (⏃) at heating rates at 10–25 ◦C/min.

HAADF - STEM

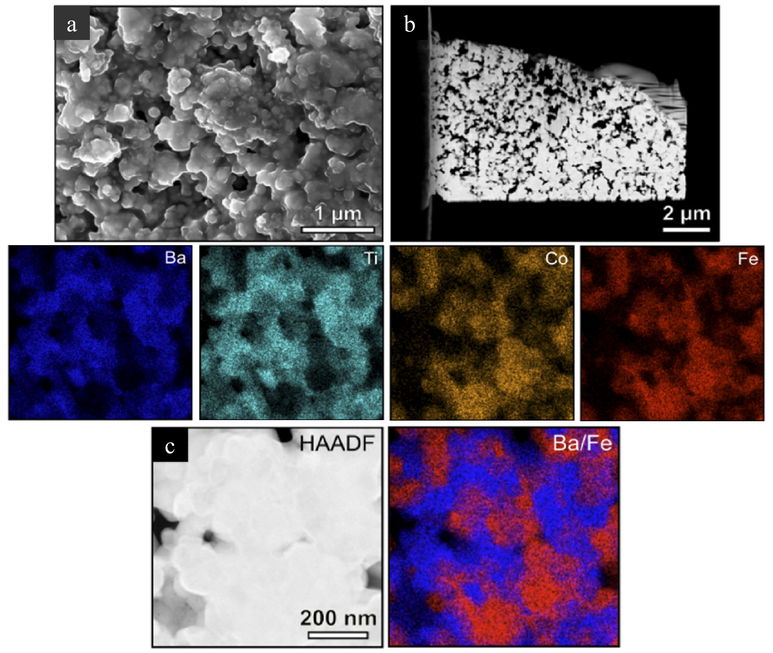

Fig. 4. Structure and composition of $BaTiO_3$/$CoFe_2O_4$ agglomerates after combustion. (a) SEM image of the agglomerate; (b) HAADF-STEM image of a cross-sectional FIB lamella (c) - HAADF-STEM image and STEM-EDX mapping of the cross-sectional lamella. A Ba/Fe overlaid STEM-EDX map is also shown.

X-Ray Profile

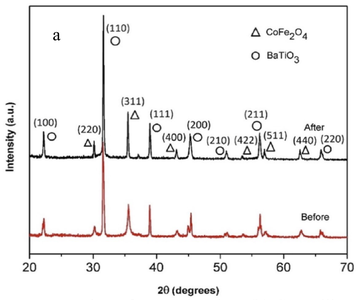

- XRD suggests original structures are mostly preserved after CCSO and carbon is not incorporated into the final product. XRD peaks are sharper and more intense after combustion, suggesting an increase in size and crystallinity.

b	Size $BaTiO_3$ (nm)	Size $CoFe_2O_4$ (nm)
Before	41.6	32.5
After	63	71.8

Fig. 5. (a) X-Ray diffractions before and aftercombustion. Both the initial and final products are comprised of tetragonal BaTiO3 and cubic CoFe2O4 phases without any trace of secondary and carbide phases in the composites after combustion. (b) Crystallite sizes in the mixture before and after combustion were estimated Using Scherrer's Formula $\frac{k\lambda}{\beta cos\theta}$ where k= 0.94, λ = 1.54 Å, and β is the average of the corrected FWMH in radians of the peaks.

Magnetoelectric Characterization

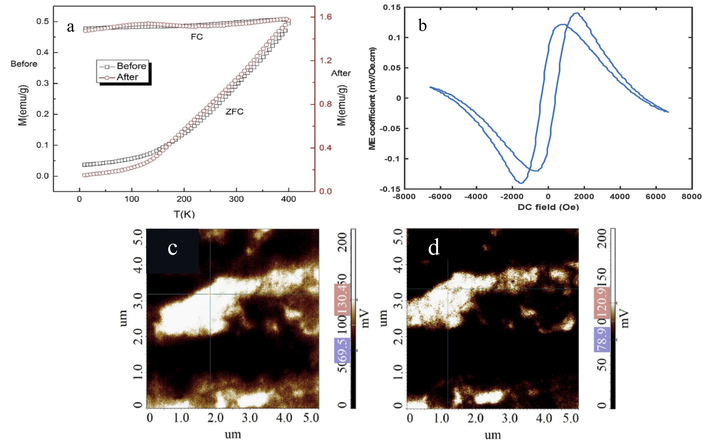

Fig. 6. (a) Temperature dependence of magnetization curves suggest that particles are of typical ferromagnetic nature. (b) Shows that there is an an electric response of when a magnetic field to the material. This behavior can be explained to the geometrical piezoelectricity of $BaTiO_3$ where conducting lattices are in contact allowing current to flow under the strain of the magnetic field. Further constriction results in decoupling of the conducting lattices. (c) Shows the surface potential of the material when no magnetic field is applied, and in (d) a 50 Oe field is applied and the surface potential decreases. This suggests rearrangement of the magnetic domains in the prescence of a magnetic field having an effect in the electrical conductance of the sample.

Conclusions

- This study proved feasible to synthesize a ferrite-ferroelectric system matrix structure with magnetoelectric coupling by using CCSO with minimal damage to the initial structure of the materials. The determining parameters for product synthesis are the carbon concentration in the reagent mixture and oxygen pressure.
- The thermodynamic calculations suggest that the mixture containing n=2-4.5 carbon can generate liquid phases which will aid in the coupling of materials. The calorimetry data suggests that the n=4.5 carbon is highly exothermic with 1430J/g energy release. The activation energy for the transition to liquid phases is at 112kJ/mol as denoted by the Arrhenius plot.
- STEM imaging of the cross-sectional FIB lamella shows the sintering of the particles in the system.
- The AFM measurements show that the particles under magnetic field become better electrical conductors. ZFC and FC measurements shows that there is a magnetoelectric coupling, suggesting that multiferroic BaTiO3–CoFe2O4 composite can be synthesized by CCSO. Magnetoelectric coupling is further confirmed by direct measurement of the magnetoelectric coefficient of pallets formed from the CCSO product under application of external magnetic field. The highest magnetoelectric coefficient observed was 0.14 mV/Oe-cm.

Acknowledgements

- We would like to acknowledge the financial support for this research by National Science Foundation (NSF) PREM (award DMR-1523577: UTRGV-UMN Partnership for Fostering Innovation by Bridging Excellence in Research and Student Success) and NSF CBET-1928334 grant. J. T.H. and K.A.M. acknowledge support from the NSF MRSEC program under Awards DMR-1420013 and DMR-2011401. STEM analysis was performed in the Characterization Facility of the University of Minnesota, which receives partial support from the NSF through the MRSEC program.

References: [1] De Leo, C. Trevino, et al. "Carbon combustion synthesis of Janus-like particles of magnetoelectric cobalt ferrite and barium titanate." *Ceramics International* (2020). [2] R.E. Lu, K.G. Chang, B. Fu, Y.J. Shen, M.W. Xu, S. Yang, X.P. Song, M. Liu, Y. D. Yang, Magnetic properties of different CoFe2O4 nanostructures: nanofibers versus nanoparticles, J. Mater. Chem. C. (2014), https://doi.org/10.1039/ c4tc01415d. [3] C. Schmitz-Antoniak, D. Schmitz, P. Borisov, F.M.F. De Groot, S. Stienen, A. Warland, B. Krumme, R. Feyerherm, E. Dudzik, W. Kleemann, H. Wende, Electric in-plane polarization in multiferroic CoFe2O 4/BaTiO3 nanocomposite tuned by magnetic fields, Nat. Commun. (2013), https://doi.org/10.1038/ ncomms3051. [4] K.S. Martirosyan, D. Luss, Carbon combustion synthesis of complex oxides: process demonstration and features, AIChE J. (2005), https://doi.org/10.1002/aic.10528. [5] K.S. Martirosyan, D. Luss, Carbon combustion synthesis of Ferrites: synthesis and characterization, Ind. Eng. Chem. Res. 46 (2007) 1492, https://doi.org/10.1021/ ie060571l. [6] K.S. Martirosyan, L. Chang, J. Rantschler, S. Khizroev, D. Luss, D. Litvinov, Carbon combustion synthesis and magnetic properties of cobalt ferrite nanoparticles, IEEE Trans. Magn. 43 (6) (2007) 3118, https://doi.org/10.1109/TMAG.2007.893844. [7] K.S. Martirosyan, E. Galstyan, S.M. Hossain, Y.J. Wang, D. Litvinov, Barium hexaferrite nanoparticles: synthesis and magnetic properties, mater. Sci. Eng. B solid-state mater, Adv. Met. Technol. (2011), https://doi.org/10.1016/j. mseb.2010.08.005. [8] K.S. Martirosyan, C. Dannangoda, E. Galstyan, D. Litvinov, Screen-printing of ferrite magnetic nanoparticles produced by carbon combustion synthesis of oxides, J. Appl. Phys. (2012), https://doi.org/10.1063/1.4711097.